RSC Advances

PAPER

View Article Online
View Journal | View Issue

Cite this: RSC Adv., 2014, 4, 36316

Catalytic performance of Au^{III} supported on SiO_2 modified activated carbon

Xiaohui Tian, Guotai Hong, Ying Liu, BinBo Jiang* and Yongrong Yang

Received 21st June 2014
Accepted 7th August 2014

DOI: 10.1039/c4ra06068g

www.rsc.org/advances

Silica was deposited onto activated carbon through TEOS hydrolysis and this composite was used as a support for the Au catalyst in acetylene hydrochlorination. Silica content and the catalyst synthesis process were both optimized. It was found that 1Au/5SiO_2/AC showed improved stability, while being as active as 1Au/AC. Thermogravimetric analysis (TGA) quantitatively revealed the synchronism of TEOS hydrolysis and Au deposition, which was believed to be the linchpin in 1Au/5SiO_2/AC synthesis. Scanning electron microscopy (SEM) and X-ray diffraction (XRD) demonstrated that amorphous silica dispersed on the carbon surface uniformly as spherical particles. Silica deposition brought down the surface area of the catalyst while leading to better distribution of gold nanoparticles. Higher gold distribution degree guaranteed the catalytic activity of 1Au/5SiO_2/AC despite surface area loss. A higher level of resistance to acetylene, excellent surface property stability and less carbonaceous deposition were determined as the origin of the improved stability of 1Au/5SiO_2/AC.

Introduction

The manufacture of the vinyl chloride monomer (VCM) *via* $HgCl_2$ catalyzed acetylene hydrochlorination is an important industrial route, contributing nearly twenty percent of global poly-vinyl chloride production and more than sixty percent of that in China.[1] Nowadays, rekindled enthusiasm in coal-derived feedstock makes this route economically more advantageous than ethylene oxychlorination, the major route for VCM production around the globe. Unfortunately, manipulation of the industrial catalysts is quite complicated and dangerous, as the catalysts, mainly consist of mercuric chloride and activated carbon, deactivate rapidly owing to the volatility of highly toxic mercuric compounds.[2,3] Extensive environmental concerns arise and the quest for alternatives never ceases.

Topics of gold nanostructured catalysts have augmented exponentially in the last 20 years due to their potential applicability to various reactions of industrial and environmental interest.[4–8] In 1990s, carbon supported Au^{III} has been identified as the most active catalyst for acetylene hydrochlorination and the investigation continues.[9–11] High price of gold makes two functionalities, the catalytic activity and stability, particularly important in acetylene hydrochlorination. Despite its high price, gold catalyst is feasible in industry since it is easy to be retrieved as other noble metals (Pd and Pt, for instance). Actually, lifetime of the catalyst was much more crucial for application. Gold catalyst in acetylene hydrochlorination undergoes slow deactivation, which can be correlated to reduction of Au^{III}, carbonaceous deposition,[10] loss of surface area and sintering of Au nanoparticles.[12] Past researches comprise two main ways in solving this problem. Firstly, Hutchings, Conte and coworkers have paid general attention on prolongation of the life time of gold catalyst through regeneration of it. Unlike mercury-based catalyst, gold based catalyst in acetylene hydrochlorination never deactivates due to run off of gold element. Only very slight gold loss (less than 1%) was detected by Hutchings[9] and Zhang,[13] which is considered as the basis of regeneration. Furthermore, it was demonstrated that treatment of deactivated gold catalyst by aqua regia could restore its activity without any gold loss, thus making multiple cycles of deactivation/regeneration possible.[14,15] In account of these findings, Conte and coworkers proposed aqua regia as an effective and economical regenerating reagent. However, despite its effectiveness, the offline regeneration process was not preferred for application, let alone the complexity of aqua regia in operation. Besides of this offline way, more attention was given to additives, metal salts mostly, that can improve the catalytic stability.[12,13,16,17] Gold in combination with additional metal salts sometimes resulted in higher catalytic activity as well as better stability. Among various alternate elements, it seems that copper, congener of gold, is the best one. In addition, Co [12] and La [13] showed benefits in Au^{III} reduction and coke deposition resistance. Generally speaking, the screening of a second metal is relatively inefficient and in lack of instructive theories.

By far, activated carbon is determined as the unique support for gold species in acetylene hydrochlorination. Although oxide supports, such as SiO_2, Al_2O_3 and TiO_2, are playing an increasingly important role in modern catalysis owing to their

---

State Key Laboratory of Chemical Engineering, Department of Chemical and Biochemical Engineering, Zhejiang University, Hangzhou 310027, P. R. China. E-mail: jiangbb@zju.edu.cn

versatile properties, they are unviable for hydrochlorination because TOFs (turnover frequency) are very low after gold being supported on them.[9,12] By contrast, in the most attractive application of gold catalyst, low temperature CO oxidation, oxide supports are crucial and versatile. It is known that the function of different oxide supports in CO oxidation varies. For example, Au/SiO_2 exhibits very low activity and good stability; meanwhile Au/TiO_2 is highly active but suffers deactivation upon calcination.[18] To unite the superiorities of different oxide materials, composite oxide supports have been finely designed for CO oxidation catalysts, leading to a more profound understanding of gold–support interaction, and also rendering a reference method for other catalytic systems as well. Plenty of literatures have reported improved performance of noble metal catalysts on composite supports.[19–23]

This prompted us to perform a systematic study of the function of composite supports for hydrochlorination of acetylene, since support is one of the most important aspects in heterogeneous catalysis. In this contribution, we report the potential of composite support in acetylene hydrochlorination for the first time. Silica modified activated carbon was used as support for gold to investigate effect of carbon modification by oxides. Properties of these catalysts were characterized by scanning electron microscopy (SEM), nitrogen adsorption isotherms (BET), transmission electron microscopy (TEM), thermal gravimetric analysis (TGA) and X-ray diffraction (XRD). This work provides an example for catalyst design and may be helpful to broaden researchers' methodological horizons in hydrochlorination.

Experimental

Materials and reagents

$HAuCl_4 \cdot 4H_2O$ (assay 49%) and C_2H_5OH were purchased from Guoyao Chemical Reagent Company (Shanghai, China); activated carbon (marked as AC, 20–40 mesh) was obtained from Jiangsu Yonghua Fine Chemicals Co., Ltd.; tetraethyl orthosilicate (TEOS) was purchased from Hangzhou Shuanglin Chemical Reagent Factory. Hydrogen Chloride (99.998%) was provided by Shanghai Weichuang Standard Gas Analytical Technology Co., Ltd.; acetylene (99.5%) was purchased from Jiaxing Tianli Gas Co., Ltd.

Catalyst preparation

The activated carbon was initially washed with dilute aqueous HCl (1 mol L^{-1}) at 70 °C for 5 h to remove residual alkali species, which may affect the distribution of nanoparticles on the support. This mixture was filtered, washed with distilled water till pH = 7 and then dried at 140 °C for 12 to 18 h.

In all samples introduced in the following paragraphs, Au content was controlled at 1% in weight, denoted as 1Au. SiO_2 content of the catalyst was denoted as $x$$SiO_2$ (*e.g.* 5SiO_2 means SiO_2 mass ratio of the sample was 5%).

The activated carbon-supported gold catalyst (Au/AC) was prepared according with the incipient wetness impregnation technique. Proper amount of $HAuCl_4$ aqueous solution was added dropwise to the activated carbon support under shaking. After that, the wet product was kept at room temperature for 2 h to gain a better impregnation, and then dried at 140 °C for 18 h before being collected for use.

SiO_2 modified activated carbon (SiO_2/AC) was prepared by impregnation of tetraethyl orthosilicate (TEOS) dissolved in ethanol (TEOS : ethanol = 1 : 15, mass ratio). The volume of the solution was approximately 3.2 times that of the total pore volume of the activated carbon. The solution was further added dropwise to the acid-washed carbon under shaking. After that, the wet product was kept at room temperature for 1 h in vacuum (−95 kPa) and then dried under the same vacuum degree at 60 °C for 6 h. The product was dried in air under 70 °C for 12 h. During these processes, ethanol evaporated as well as TEOS hydrolyzed to SiO_2 on activated carbon.

Au/SiO_2/AC was prepared by using collected SiO_2/AC (before exposure in air longer than 5 min) as support. Wetness impregnation was still the technique for gold supporting. Preparation of SiO_2/Au/AC involved the preparation of Au/AC in the first step and SiO_2 modification of Au/AC in the second, took the same procedures of activated carbon modification as introduced.

As a variation, two samples denoted as SiO_2(ammonia)/Au/AC and Au/SiO_2(ammonia)/AC were prepared. Difference of these two samples with Au/SiO_2/AC and SiO_2/Au/AC was that ammonia liquor (0.1 mol L^{-1}) was added dropwise to SiO_2/AC and SiO_2/Au/AC after vacuum drying under 60 °C respectively. Then, ammonia contained samples were kept at room temperature for 1 h before being dried at 70 °C for 12 h. The volume of ammonia liquor was equal to the total pore volume of the support.

Catalyst testing

Hydrochlorination reaction of acetylene was carried out in a fixed bed laboratory microreactor. Catalysts were tested using a stainless steel reactor tube (i.d. of 8 mm). The reaction zone consisted of 1.0 g fresh sample of catalyst. The reactor was operated at atmospheric pressure, and maintained at 180 °C, in down-flow mode. N_2 was used as purging gas. The pressure of the reactants, HCl and C_2H_2, was chosen for safety and in accordance with industrial operating condition.

After being heated to 180 °C, highly purified hydrogen chloride was regulated by mass flow controllers and fed into the reactor alone for 1 h to activate the catalyst, according to the industrial process. Then, acetylene was introduced into concentrated sulfuric acid to remove trace poisonous impurities such as acetone, moisture, S, P and As, and subsequently fed into the reactor to start the reaction.

A total GHSV of 530 h^{-1} was chosen to determine the optimal catalyst preparation procedure. Catalytic stability and the effect of SiO_2 content on catalytic performance were tested under a higher GHSV of 1060 h^{-1}. Conversion of acetylene was not too high in both situations. Thus all results obtained were in the kinetic regime. The gas product was passed through a vessel filled with 15% sodium hydroxide solution and a drying tube in sequence to remove the remaining hydrogen chloride and moisture. The composition of the effluent was determined immediately using a gas chromatography equipped with a flame ionization detector. Two catalytic functionalities of the catalysts, conversion of acetylene (X_A) and the deactivation rate (DR), were defined as follows:

$$X_A = (1 - \varphi_A) \times 100\% \tag{1}$$

$$\mathrm{DR} = (X_A^L - X_A^H)/t \tag{2}$$

where φ_A is the volume fraction of remaining acetylene in gas product, X_A^L and X_A^H refer to the highest and the last X_A obtained respectively during the experiment. Time span from X_A^H to X_A^L is denoted as t, in units of hour. Selectivity of catalyst was defined as published reports.[13]

Catalyst characterization

Morphology of different catalysts were obtained by scanning electron microscopy (SEM) using a Hitachi TM-1000 scanning electron microscope (low magnification) and a Hitachi S-4700 field emission scanning electron microscope (high magnification). The samples were deposited on carbon holders and evacuated at high vacuum before micrographs were taken.

The texture properties of the catalysts were derived from N_2 adsorption–desorption measurements carried out at liquid nitrogen temperature using an ASAP2020 instrument. Prior to any adsorption measurements, each sample was outgassed at 200 °C for 6 h to eliminate air and vapor from the capillaries of the pore structures of the solids. Specific surface areas and pore volume of the samples were calculated applying BET and *T*-plot models respectively.

The crystal structures were studied with a Philips PW3050/60 vertical goniometer using Ni-filtered Cu Kα radiation ($\lambda = 1.5406$ Å). A proportional counter and a 0.02° step size in the 2θ range from 5 to 80°. The assignment of the various crystalline phases was based on the JPDS powder diffraction file cards.

To determine SiO_2 content and the content of carbonaceous deposits on catalysts after reaction, samples were analyzed thermogravimetrically (TA Instruments, TGA2050). Analysis was performed under flowing air from 50 °C to 750 °C with a flow rate of 50 cm^3 min^{-1}, and a heating rate of 10 °C. Differential thermogravimetric analysis (DTGA) curves were obtained from the TGA data by numerically differentiating the later with respect to temperature.

Transmission electron microscopy (TEM) studies were performed on Tecnai F20 instrument operating at 120 kV to study the distribution of Au nanoparticles. The ground catalysts were dispersed in ethanol and then supported on a copper grid.

Results and discussion

Effect of synthesis process and SiO_2 content on catalytic performance

Catalytic performance of different samples, namely 1Au/AC, 1Au/5SiO_2/AC, 5SiO_2/1Au/AC, 1Au/5SiO_2(ammonia)/AC and 5SiO_2(ammonia)/1Au/AC, were tested. Conversion of acetylene for each catalyst is plotted against the time on stream (TOS) in Fig. 1.

It was observed that whilst the highest catalytic activities of 1Au/5SiO_2/AC and 1Au/5SiO_2(ammonia)/AC were both close to activity of 1Au/AC, 5SiO_2/1Au/AC and 5SiO_2(ammonia)/1Au/AC showed relatively low activities. For 5SiO_2/1Au/AC, might it be the case that modification of 1Au/AC resulted in coverage of active species by SiO_2, which made them not readily available to reactants. Additionally, ammonia liquor added during synthesis of 5SiO_2(ammonia)/1Au/AC promoted the hydrolysis of TEOS, hence resulting in more SiO_2 covering gold nanoparticles. Ammonia liquor could reduce Au^{III} to metallic gold in the meantime. Synergetic effects of active site coverage and reduction of Au^{III} brought the catalytic activity of 5SiO_2(ammonia)/1Au/AC down to a significantly lower level than 5SiO_2/1Au/AC, as shown in Fig. 1. Furthermore, it seemed that the induction period of catalyst was also related to catalyst synthesis procedures. Both of 5SiO_2/1Au/AC and 5SiO_2(ammonia)/1Au/AC showed a markedly slower approach to steady-state activity, which was not preferred, whilst 1Au/AC, 1Au/5SiO_2/AC and 1Au/5SiO_2(ammonia)/AC reached to steady-state activity in two hours.

Another important catalytic property affected by SiO_2 modification was stability. According to Fig. 1, distinction of 1Au/AC, 1Au/5SiO_2/AC and 1Au/5SiO_2(ammonia)/AC was more obvious in stability than in activity. As defined by eqn (2), deactivation rates of 1Au/AC and 1Au/5SiO_2(ammonia)/AC were -0.88% h^{-1} and -0.84% h^{-1} respectively. By contrast, 1Au/5SiO_2/AC deactivated at -0.35% h^{-1}, a significantly slower rate in comparison with the previous two samples.

The synthesis process of 1Au/SiO_2/AC was accordingly chosen as the best one and a question immediately emerged: following this process, what value of SiO_2 content was preferred? To answer this question, further experiments were performed and results are displayed in Fig. 2. 1Au/1SiO_2/AC and 1Au/10SiO_2/AC were prepared and tested under a total GHSV of 1060 h^{-1}. In comparison, 1Au/AC and 1Au/5SiO_2/AC were prepared and tested again under this higher GHSV. As can be seen in Fig. 2, all three 1Au/$x$$SiO_2$/AC samples were more stable than 1Au/AC. According to eqn (2), 1Au/AC, 1Au/1SiO_2/AC,

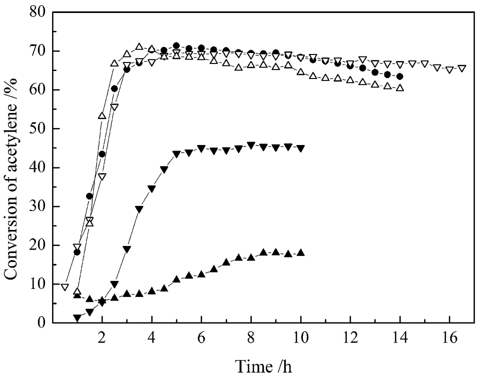

Fig. 1 Conversion of acetylene over 1Au/AC (●), 1Au/5SiO_2/AC (▽), 5SiO_2/1Au/AC (▼), 1Au/5SiO_2(ammonia)/AC (△) and 5SiO_2(ammonia)/1Au/AC (▲). C_2H_2 flow rate was 12.5 mL min^{-1}, HCl/C_2H_2 = 1.13, GHSV = 530 h^{-1}.

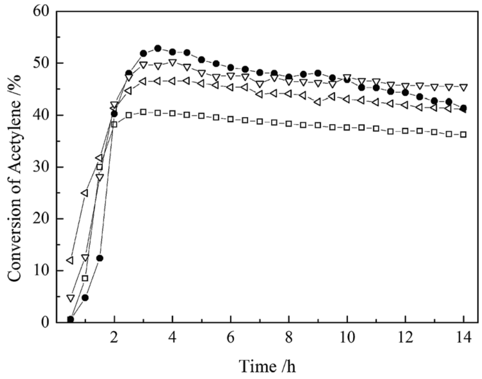

Fig. 2 Acetylene Conversion over 1Au/AC (●), $1Au/1SiO_2/AC$ (□), $1Au/5SiO_2/AC$ (▽), $1Au/10SiO_2/AC$ (◁), C_2H_2 flow rate was 25 mL min^{-1}, $HCl/C_2H_2 = 1.13$, GHSV = 1060 h^{-1}.

$1Au/5SiO_2/AC$ and $1Au/10SiO_2/AC$ deactivated at $-1.09\ h^{-1}$, $-0.40\ h^{-1}$, $-0.48\ h^{-1}$ and $-0.57\ h^{-1}$ respectively. Length of the induction period of all samples was close to each other. The most active sample was $1Au/5SiO_2/AC$ as well $1Au/1SiO_2/AC$ the least active one. Although more stable than $1Au/5SiO_2/AC$, $1Au/1SiO_2/AC$ showed a much lower activity, which was not preferred in the comparative study of this article. On the other hand, all catalysts showed high selectivity toward VCM (>99.7%). Considering all these factors, namely, catalytic activity, stability, selectivity and induction period, we concluded that the optimal procedure in SiO_2 modification is the one followed to synthesize $1Au/5SiO_2/AC$. The rest of this contribution was performed to figure out differences between 1Au/AC and $1Au/5SiO_2/AC$.

Hydrolyzing time of TEOS and amount of SiO_2 formed along with gold impregnation

It is worth noting that large stability variation between $1Au/5SiO_2/AC$ and $1Au/5SiO_2$(ammonia)/AC exists, which might root in their difference of TEOS hydrolyzing time. Reasonably, we assumed that during the synthesis process of $5SiO_2/AC$ TEOS was not completely hydrolyzed in absence of hydrolytic agent. Moreover, there must be some TEOS remained on $5SiO_2/AC$ after heating under 70 °C because of its high boiling point (165.5 °C). Addition of ammonia liquor to $5SiO_2/AC$ might help accomplish TEOS hydrolysis. Consequently, during the synthesis process of sample $1Au/5SiO_2$(ammonia)/AC, hardly any SiO_2 formed when gold nanoparticles deposition took place in the subsequent step and weak interaction between them happened. On the contrary, during the synthesis process of sample $1Au/5SiO_2/AC$, addition of acidic $HAuCl_4$ solution onto $5SiO_2/AC$ promoted formation of SiO_2 simultaneously with gold nanoparticles deposition, thus facilitating more immediate impaction between them.

This was testified quantitatively by analysis of TGA results through calculating mass ratio of inert (non-combustible) solid residue after burning under 750 °C. Fresh activated carbon, $5SiO_2/AC$ (immediately analyzed after 12 h drying at 70 °C) and corresponding $1Au/5SiO_2/AC$ were analyzed for four times respectively to gain an average residue mass ratio for each sample, as shown in Table 1 and Fig. 3. As listed in Table 1, fresh activated carbon contained 2.77 wt% of non-combustible materials, while it was 1.78 wt% higher for $5SiO_2/AC$ due to deposition of SiO_2. Moreover, the mass ratio of inert residue grew to 7.46 wt% for $1Au/5SiO_2/AC$, which consisted of non-combustible materials on activated carbon (2.77 wt%), gold loaded on the carbon (1.0 wt%) and deposited SiO_2. Thus, SiO_2 content on $1Au/5SiO_2/AC$ was calculated as 3.69 wt%, with 1.91 wt% of that formed during Au^{III} impregnation (subtract the mass ratio of SiO_2 on $5SiO_2/AC$). In comparison with $1Au/5SiO_2$(ammonia)/AC, we believe that it might be this part of SiO_2 that enhanced stability of $1Au/5SiO_2/AC$. Moreover, no significant difference on TGA and DTGA profiles between 1Au/AC and $1Au/5SiO_2/AC$ is observed from Fig. 3, indicating that SiO_2 doesn't interact with carbon strongly.

Table 1 Inert residue mass ratio of support and silica doped samples

	1	2	3	4	Mean residue wt%	SiO_2 Content wt%
AC	2.7	2.72	3.12	2.53	2.77	0
$5SiO_2/AC$	4.55	4.45	4.68	4.51	4.55	1.78
$1Au/5SiO_2/AC$	7.73	6.24	8.80	7.06	7.46	3.69

It is intriguing to note the advantage of this synchronism over cases that SiO_2 deposited before or after Au impregnation. It seems that SiO_2 formation during $HAuCl_4$ impregnation could tune the final distribution of gold species, through interaction among TEOS, SiO_2 and aqueous solution. Probably, besides selection of proper modifiers, of particular importance for catalyst design is how depositing gold species interact with the modifiers at carbon surface. This inclination is the same as strong acid (such as aqua regia), which favors support modifying (by acid) simultaneously with gold impregnation,[14] implying the importance of "synchronism effect" in gold catalyst exploration.

Morphology of SiO_2 on the catalysts and its crystal form

The morphology of 1Au/AC, $5SiO_2/AC$ and $1Au/5SiO_2/AC$ was characterized by scanning electron microscopy. SEM images are

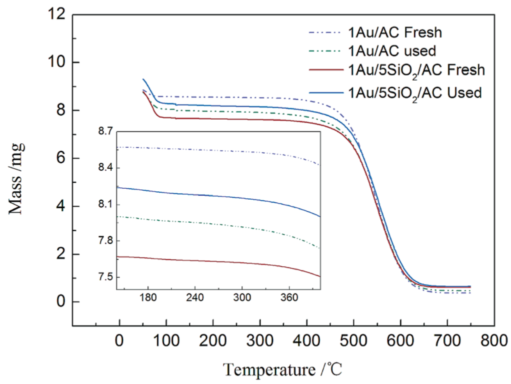

Fig. 3 TGA and DTGA profiles of AC, 1Au/AC, $5SiO_2/AC$ and $1Au/5SiO_2/AC$.

presented in Fig. 4 at different magnifications. Low magnification (1000×) images reveal that SiO_2 distributes as micro-sized particles on the surface of activated carbon (Fig. 4(a)). Image of $1Au/5SiO_2/AC$ (Fig. 4(c)) clearly demonstrates that SiO_2 particle has a dense and uniform dispersion, which surely will alter the property of activated carbon. In the meantime, a sparser distribution was observed on the surface of $5SiO_2/AC$ (Fig. 4(b)), indicating a lower content of SiO_2. To our knowledge, TEOS slowly hydrolyzed along with ethanol's evaporation during the preparation of $5SiO_2/AC$. Without promotion of water, acid or base, hydrolysis of TEOS in $5SiO_2/AC$ was incomplete. The remained TEOS hydrolyzed quickly after addition of aqueous solution of $HAuCl_4$, hence resulting in the denser distribution of SiO_2 particles on the surface of $1Au/5SiO_2/AC$. High magnification (15K×) SEM micrograph (Fig. 4(d)) depicted the specific appearance of SiO_2 particles. Most of SiO_2 particles immobilized on the surface of activated carbon had a near-spherical shape, with diameters of 100 nm–1 μm.

X-ray diffraction was conducted to determine crystal form of SiO_2 on the catalyst. The powder XRD patterns of AC, 1Au/AC, $5SiO_2/AC$, $1Au/5SiO_2/AC$, $10SiO_2/AC$ and $1Au/10SiO_2/AC$ are displayed in Fig. 5.

The broad peak in the range of $2\theta = 15$–$30°$ in fresh activated carbon XRD pattern reflects the amorphous structure of the support. Slight intensity growth of that broad peak can be observed from the sample containing no SiO_2 to 10% SiO_2 deposited sample, providing evidence for the formation of amorphous silica only as no peaks for other SiO_2 crystal forms were observed. Compared $1Au/5SiO_2/AC$ to $5SiO_2/AC$, the slight peak increase again testified a SiO_2 content elevation after Au^{III} impregnation. In the XRD of 1Au/AC, $1Au/5SiO_2/AC$ and $1Au/10SiO_2/AC$, intensive diffraction patterns at $2\theta = 38°$, 44.8°, 65° and 77.5° agree well with metallic gold peaks. These peaks, being assigned to the (111), (200), (220) and (311) planes of the crystalline FCC structure of gold, imply that reduction of Au^{III} happens in the process of catalyst preparation.

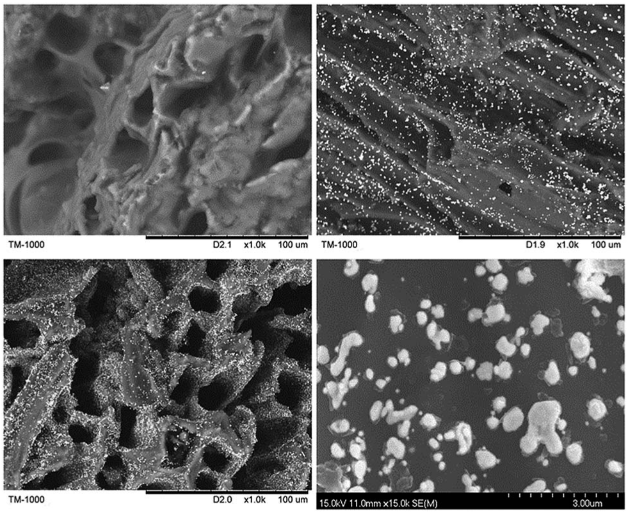

Fig. 4 SEM images of AC (a), $5SiO_2/AC$ (b) and $1Au/5SiO_2/AC$ (c and d).

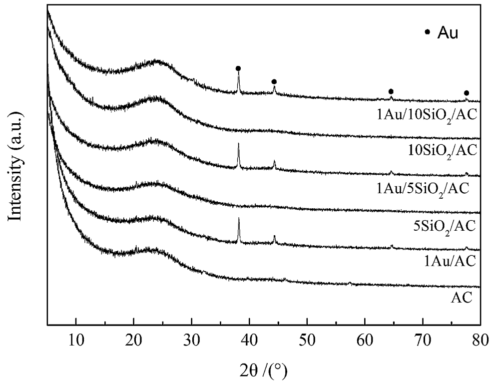

Fig. 5 XRD patterns of different samples.

Influence of SiO_2 modification on carbon surface and surface stability of the $1Au/5SiO_2/AC$

BET results of different samples are listed in Table 2. The total surface area of activated carbon was 1180 $m^2\ g^{-1}$. It increased slightly to 1201 $m^2\ g^{-1}$ after impregnation of $HAuCl_4$, which might be resulted from bridging of $HAuCl_4$ crystals in 1Au/AC. After being modified by SiO_2, the surface area of $5SiO_2/AC$ slightly dropped to 1111 $m^2\ g^{-1}$. Meanwhile, $1Au/5SiO_2/AC$ possessed a significantly lower surface area of 963.7 $m^2\ g^{-1}$, which was only 80% of 1Au/AC and 88% of $5SiO_2/AC$. The difference of surface area between $5SiO_2/AC$ and $1Au/5SiO_2/AC$ is in coincident with results introduced above since more SiO_2 formed on $1Au/5SiO_2/AC$.

Ratio of micropore area was 46.1% for activated carbon. Deposited gold nanoparticles on 1Au/AC reduced this ratio to 42.8%, implying micropores as slightly preferred position for anchoring of nanoparticles. Higher micropore area ratio of $1Au/5SiO_2/AC$ (45.2%) hinted the formation of micropores on/among SiO_2 particles, or between SiO_2 spheres and activated carbon framework.

Beside of the difference of surface area and micropore area of fresh samples, significant disparity between 1Au/AC and $1Au/5SiO_2/AC$ was observed after hydrochlorination reaction. As shown in Table 2, surface area of 1Au/AC greatly reduced to 1071 $m^2\ g^{-1}$ after 14 h on stream, about 11% lower than that of fresh sample. Micropore area followed almost the same trend. On the contrary, only 2.88% loss of surface area happened within the same time for $1Au/5SiO_2/AC$. Loss of micropore area was only 2.76% in the meantime. Similar trend was observed for pore volume, micropore volume and average pore diameter. As is well known, the loss of surface area is mainly because of collapse and sealing of pores of the catalyst. This blockage isolated active sites in those pores from reactants and made the catalyst less active. According to results listed in Table 2, superior surface stability of $1Au/5SiO_2/AC$ is considered to be one of the most important factors in maintaining catalytic activity compared to 1Au/AC. This might stem from the strengthening of surface channels by uniformly distributed SiO_2 particles, which protected pores from collapse.

Table 2 BET results of AC, 1Au/AC, $5SiO_2$/AC, 1Au/$5SiO_2$/AC and corresponding used samples[a]

		1Au/AC		$5SiO_2$/AC	1Au/$5SiO_2$/AC	
Catalysts	AC	Fresh	Used	Fresh	Fresh	Used
Surface area (a)	1184.8	1201	1071.8	1111	963.7	935.9
Micropore area (a)	546.7	513.9	445	452.2	436	424
Ratio of micropore area	0.461	0.428	0.415	0.407	0.452	0.453
Pore volume (b)	1.093	1.124	1.028	1.039	0.915	0.903
Micropore volume (b)	0.28	0.26	0.22	0.23	0.22	0.22
Ave. pore diameter (c)	3.69	3.74	3.84	3.74	3.80	3.86

[a] Units in the table: (a) $m^2\ g^{-1}$, (b) $cm^3\ g^{-1}$, and (c) nm.

Gold dispersion in catalysts and its thermal resistance ability

As aforementioned, catalytic activity of 1Au/$5SiO_2$/AC is nearly the same with 1Au/AC while being grossly inferior in surface area. This phenomenon can be explained by TEM observed smaller nanoparticles on 1Au/$5SiO_2$/AC, as presented in Fig. 6.

No large particles, several tens of nanometers in diameter, were observed on fresh 1Au/$5SiO_2$/AC and 1Au/AC. Nanoparticles on 1Au/AC are in the range between 5.0 to 17.3 nm, with an average diameter of 11.1 nm. In the case of 1Au/$5SiO_2$/AC, gold particles are in the range between 2.0 and 9.3 nm, mean size of which is 5.4 nm. Standard deviation of particle diameter is 2.7 nm for 1Au/AC and 1.5 nm for 1Au/$5SiO_2$/AC separately. It is clear that SiO_2 modification leads to improved distribution of active sites and hence compensates its disadvantage in surface area.

Spent catalysts of 1Au/AC and 1Au/$5SiO_2$/AC after 14 h on-stream testing (Fig. 2) have also been analyzed to observe the particle sintering. Intensive sintering of gold nanoparticles was observed in both samples. Whilst much less number of small nanoparticles could be discerned, particles with a diameter of ~100 nm or more were observed. Obvious sintering observed in our samples is quite different with Conte's work, in which no obvious sintering was observed,[11] possibly because of the difference between selected activated carbon supports.

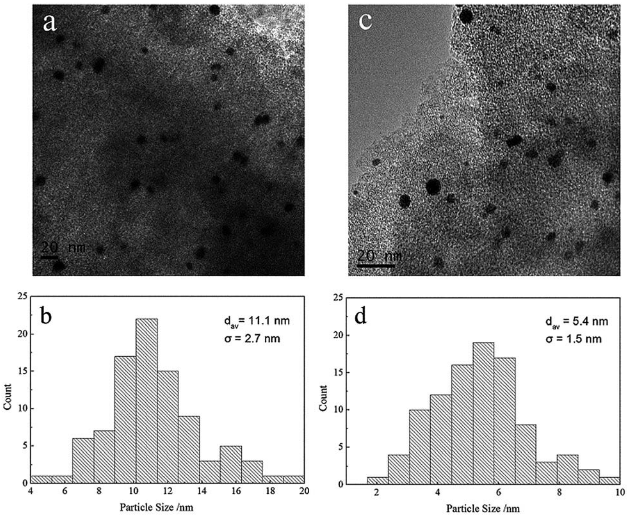

Fig. 6 TEM images and particle size distributions of fresh 1Au/AC (a and b) and 1Au/$5SiO_2$/AC (c and d).

Severe sintering made the statistics of particle size for spent catalysts impossible and undependable because reliability of TEM statistical results is dependent on the uniformity of bulk samples. Accordingly, two experiments were performed to estimate the difference of sintering between 1Au/AC and 1Au/$5SiO_2$/AC. In both experiments, fresh samples of 1Au/AC and 1Au/$5SiO_2$/AC were placed in an oven at 180 °C under N_2 protection for 32 h respectively before activity testing under 1060 h^{-1}. It can be reasonably assumed that no surface property change took place during this period on account of that the production of activated carbon involves calcination of raw materials under greatly higher temperature (around 800 °C) for hours. Moreover, Conte has demonstrated that simple thermal treatment at 180 °C in absence of C_2H_2/HCl reactants could not alter the valence state of gold.[16] And of course, carbonaceous deposition did not happen since no reaction took place. Accordingly, activity loss after thermal treatment can be solely ascribed to sintering of gold nanoparticles. Steady-state activity of both fresh 1Au/AC and 1Au/$5SiO_2$/AC without thermal treatment during this test were 48.3% and 46.7% respectively (Fig. 7(a)), slightly lower than in Fig. 2 as catalyst for each test was newly prepared and there do exist some labile factors during pore volume impregnation, which cannot be eliminated totally because of its shortcoming. However, activity disparity between 1Au/AC and 1Au/$5SiO_2$/AC changed little. Thus the results were believed to be reliable. As shown in Fig. 7(b), compared to analogous sample without 32 h thermal treatment, highest conversion of acetylene after thermal treatment was 45.6% for 1Au/AC, dropped by 5.6% relatively. For 1Au/$5SiO_2$/AC, the conversion was about 42.7% and dropped by 9.4% relatively. This discrepancy indicated that smaller gold nanoparticles in 1Au/$5SiO_2$/AC that possess higher surface energy were more tended to sinter through migration and coalescence, or Ostwald ripening, than that in 1Au/AC. Obvious sintering of nanoparticles were observed too when we tried to take TEM images of the catalysts after 32 h thermal treatment. In comparison, the biggest particles observed are ~60 nm in diameter, much smaller than the biggest particles observed in spent catalysts, hinting that the reactants play roles in sintering of nanoparticles.

It is worth noting that modification of SiO_2 led to shorter induction period of fresh 1Au/$5SiO_2$/AC. After 32 h thermal treatment, induction period of 1Au/$5SiO_2$/AC was totally

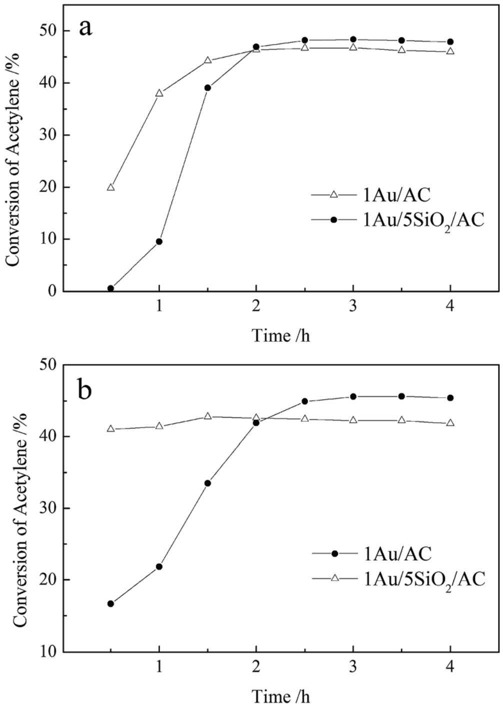

Fig. 7 Catalytic activity of 1Au/AC and 1Au/5SiO$_2$/AC: (a) fresh, (b) after 32 h thermal treatment. C_2H_2 flow rate was 25 mL min^{-1}, HCl/C_2H_2 = 1.13, GHSV = 1060 h^{-1}.

eliminated while being unchanged for 1Au/AC. This might be related to smaller gold nanoparticles in 1Au/5SiO$_2$/AC, since smaller gold nanoparticles provided more coordinatively unsaturated atoms for reactant activation. This is an issue that lacks in-depth mechanism understanding, which still needs investigation.

Acetylene resistance and roles of acetylene played in catalysis

It has been demonstrated that the reduction of Au^{III} to Au^0 in the strongly reducing conditions accompanies hydrochlorination is one of the most critical factor that deactivates the catalyst. However, Conte and coworkers showed that location of Au^{III} is more important than its content recently, which illustrates that measurement of Au^{III} content through XPS was ineffective in foreseeing activity and stability of the catalyst. Therefore, a more effective way is needed to evaluate the relative contribution of Au^{III} reduction to the loss of catalytic activity. As has been testified by Conte, acetylene is the causation of reduction of Au^{III}, whereas HCl plays a regeneration/activation role. According to this, contrast experiments were carried out to accomplish the evaluation. The catalysts, namely 1Au/AC and 1Au/5SiO$_2$/AC, were respectively exposed to switching gas circumstances in the following operating sequence:

$$C_2H_2/HCl\ (5\ h) \rightarrow HCl\ (1\ h) \rightarrow C_2H_2/HCl\ (2\ h) \rightarrow C_2H_2\ (1\ h) \rightarrow C_2H_2/HCl\ (4\ h).$$

Temperature of catalyst bed was kept at 180 °C all along, meanwhile each step of the sequence was carried out under GHSV of 1060 h^{-1}. Flow rate of HCl or C_2H_2 during HCl or C_2H_2 exposure step was set as the total reactants flow rate in an ordinary test (53 mL min^{-1}) without dilution of inactive gases. The steady-state catalytic activity after HCl or C_2H_2 exposure was measured and compared to that before the exposure, for quantitative interpretation of deactivation. We show the results in Fig. 8. It was found that before cutoff of C_2H_2 the conversion of acetylene was 46.94% for 1Au/AC and 45.46% for 1Au/5SiO$_2$/AC. This activity was maintained after 1 h pure HCl treatment for both samples (46.51% and 45.23% respectively), without obvious activation or deactivation effect being observed. By comparison, after being exposed in pure C_2H_2, the steady-state conversion of acetylene declined to 25.54% for 1Au/AC, significantly dropped by 43.1% relatively. In the meantime, the conversion of acetylene over 1Au/5SiO$_2$/AC was 26.86% after C_2H_2 exposure and only dropped by 38.0% relatively, lower than that of 1Au/AC.

Difference between 1Au/AC and 1Au/5SiO$_2$/AC after C_2H_2 exposure showed that, to some extent, SiO$_2$ strengthened C_2H_2 resistance of 1Au/5SiO$_2$/AC in comparison with 1Au/AC, thus helping maintain its catalytic activity in hydrochlorination of acetylene. These results partly verified the conclusions of Conte about effectiveness of different reactants on gold catalyst for acetylene hydrochlorination, and are helpful for catalyst design and industrial process design. Moreover, we observed that two hours were needed to reactivate each sample after C_2H_2 treatment, whereas, HCl treated samples reached steady state immediately. This phenomenon was not reported in Conte's work and implied acetylene during the exposure as a reagent that influences the catalyst not just by reducing ionic Au^{III}, which led to decreased activity (steady-state activity), but also by deteriorating the real active sites (Au^{III} containing structure that really exists in catalysis) to inactive ones (for example, coordinatively saturated Au atoms), which led to re-emergence of induction period. We envisioned this to help find a convenient way to uncover the intrinsic nature of gold catalysts for acetylene hydrochlorination in forthcoming work.

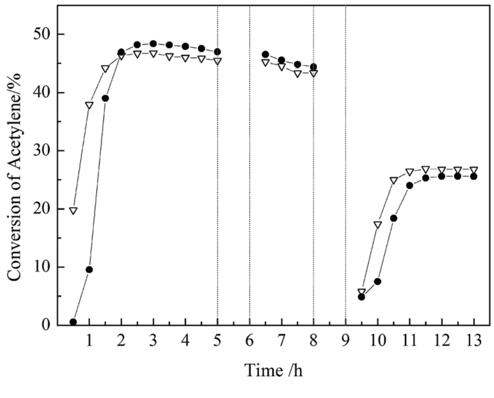

Fig. 8 Control experiments over Au/AC (●) and 1Au/5SiO$_2$/AC (▽) catalysts.

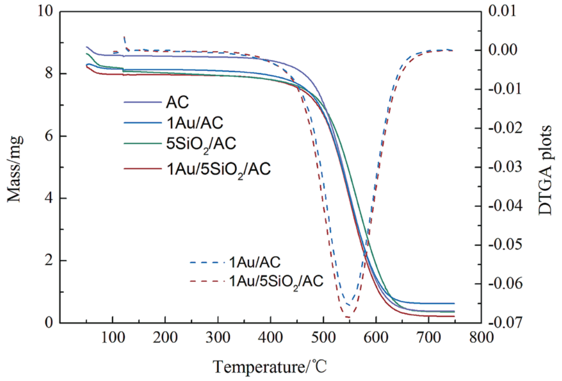

Fig. 9 TGA profiles of fresh and used 1Au/AC and 1Au/5SiO$_2$/AC catalysts.

Resistance of carbonaceous deposition after SiO$_2$ modification

Catalyst deactivation caused by site coverage and pore blockage may also be induced by growth of the carbonaceous deposits besides collapse of the channel. The amount of carbonaceous materials deposited during the reaction was determined by TGA, through subtraction of mass loss ratio between fresh and used catalysts in the temperature range 140–400 °C.[12,13] The TGA profiles of fresh/used 1Au/AC and 1Au/5SiO$_2$/AC are showed in Fig. 9. In the inset figure, it can be observed that weight loss is gradual between 140 and 400 °C. Slight growth of mass loss rate of used samples can be observed too, indicating the formation of deposits. After subtracting the values get from corresponding fresh samples, the amount of deposits formed over 1Au/AC is clearly much higher (1.593 wt%) than that over 1Au/5SiO$_2$/AC (0.719 wt%). This definitely is one of the reasons for improved stability of 1Au/5SiO$_2$/AC. The advantage in resistance of deposits formation may originate from smaller nanoparticles on 1Au/5SiO$_2$/AC, since molecules of unsaturated reactants and products adsorbed on closely contacted active sites have the tendency to polymerize with each other.

Conclusion

In this article we reported a composite support as a new orientation for gold catalysts applied in the acetylene hydrochlorination reaction. It was found that varied modification procedures of activated carbon with SiO$_2$ could influence catalytic performance in significantly different ways. Evidently, if Au^{III} impregnation took place synchronously with TEOS hydrolysis at the surface of activated carbon, good catalytic activity and stability can be achieved. The finding suggests that besides careful selection of modifiers, of particular importance for catalyst design is how depositing gold species interact with the modifiers at carbon surface—just as strong acid functions.

During the modification process, proper amount of SiO$_2$ deposition was needed. Optimized catalyst, 1Au/5SiO$_2$/AC, was studied thoroughly in comparison with 1Au/AC. SEM images revealed that amorphous SiO$_2$ spheres distributed on the surface of 1Au/5SiO$_2$/AC in a very dense mode, which substantially brought down surface area of the catalyst. However, despite this disadvantage, we found that smaller gold nanoparticles were obtained in this catalyst, thus keeping its catalytic activity as high as 1Au/AC. Furthermore, in comparison with 1Au/AC, benefits on acetylene resistance, carbonaceous deposition resistance and especially surface area stability were obtained after SiO$_2$ modification, and these finally improved the overall stability of 1Au/5SiO$_2$/AC. In summary, modification of activated carbon by SiO$_2$ could bring about stability enhancement on gold catalyst for acetylene hydrochlorination. Most significantly, 1Au/5SiO$_2$/AC showed advantages in acquisition of smaller nanoparticles and surface area stability, indicating that composite supports might have great potential in catalyst exploring for acetylene hydrochlorination.

Notes and references

1 China Chloro-Alkali Industry Association. The 12th Five-Year Plan of chloro-alkali industry in China. China Chem. Ind. News 2011, 7 (in Chinese).

2 W. Ren, L. Duan, Z. W. Zhu, W. Du, Z. Y. An, L. J. Xu, C. Zhang, Y. Q. Zhuo and C. H. Chen, *Environ. Sci. Technol.*, 2014, **48**, 2321–2327.

3 I. Trotuş, T. Zimmermann and F. Schüth, *Chem. Rev.*, 2013, **114**, 1761–1782.

4 A. S. Hashmi and G. J. Hutchings, *Angew. Chem., Int. Ed.*, 2006, **45**, 7896–7936.

5 G. J. Hutchings and M. Haruta, *Appl. Catal., A*, 2005, **291**, 2–5.

6 S. A. C. Carabineiro, L. M. D. R. S. Martins, M. Avalos-Borja, J. G. Buijnsters, A. J. L. Pombeiro and J. L. Figueiredo, *Appl. Catal., A*, 2013, **467**, 279–290.

7 E. G. Rodrigues, S. A. C. Carabineiro, J. J. Delgado, X. Chen, M. F. R. Pereira and J. J. M. Órfão, *J. Catal.*, 2012, **285**, 83–91.

8 Y. Önal, S. Schimpf and P. Claus, *J. Catal.*, 2004, **223**, 122–133.

9 B. Nkosi, N. J. Coville, G. J. Hutchings, M. D. Adams, J. Friedl and F. E. Wagner, *J. Catal.*, 1991, **128**, 366–377.

10 B. Nkosi, M. D. Adams, N. J. Coville and G. J. Hutchings, *J. Catal.*, 1991, **128**, 378–386.

11 M. Conte, A. F. Carley, C. Heirene, D. J. Willock, P. Johnston, A. A. Herzing, C. J. Kiely and G. J. Hutchings, *J. Catal.*, 2007, **250**, 231–239.

12 H. Y. Zhang, B. Dai, X. G. Wang, W. Li, Y. Han, J. J. Gu and J. L. Zhang, *Green Chem.*, 2013, **15**, 829–836.

13 H. Y. Zhang, B. Dai, X. G. Wang, L. L. Xu and M. Y. Zhu, *J. Ind. Eng. Chem.*, 2012, **18**, 49–54.

14 M. Conte, C. J. Davies, D. J. Morgan, T. E. Davies, D. J. Elias, A. F. Carley, P. Johnston and G. J. Hutchings, *J. Catal.*, 2013, **297**, 128–136.

15 M. Conte, C. J. Davies, D. J. Morgan, T. E. Davies, A. F. Carley, P. Johnston and G. J. Hutchings, *Catal. Sci. Technol.*, 2013, **3**, 128–134.

16 M. Conte, A. Carley, G. Attard, A. A. Herzing, C. J. Kiely and G. J. Hutchings, *J. Catal.*, 2008, **257**, 190–198.

17 S. J. Wang, B. X. Shen and Q. L. Song, *Catal. Lett.*, 2010, **134**, 102–109.

18 H. G. Zhu, Z. Ma, S. H. Overbury and S. Dai, *Catal. Lett.*, 2007, **116**, 128–135.

19 S. M. Park, H. Jang, E. S. Kim, H. Han and G. Seo, *Appl. Catal., A*, 2012, **427–428**, 155–164.

20 Y. Tai, J. Murakami, K. Tajiri, F. Ohashi, M. Daté and S. Tsubota, *Appl. Catal., A*, 2004, **268**, 183–187.

21 K. Nakagawa, T. Okayama, Y. Tanimoto, K. Sotowa, S. Sugiyama, T. Moriga, S. Takenaka and M. Kishida, *Appl. Catal., A*, 2012, **419–420**, 13–21.

22 K. Qian, W. X. Huang, Z. Q. Jiang and H. X. Sun, *J. Catal.*, 2007, **248**, 137–141.

23 R. J. H. Grisel, C. J. Weststrate, A. Goossens, M. W. J. Crajé, A. M. van der Kraan and B. E. Nieuwenhuys, *Catal. Today*, 2002, **72**, 123–132.